

Cockcroft-Latham Fracture Criterion and Bulk Formability of Copper Base Alloys

Cockcroft-Lathamov kriterij loma in masivna preoblikovalnost bakrovih zlitin

B. Ule*, V. Leskovšek, B. Breskvar, Institute of Metals and Technology, Ljubljana, Slovenia

K. Kuzman, D. Švetak, Faculty for Mechanical Engineering, Ljubljana, Slovenia

F. Kofol, Kolektor, Idrija, Slovenia

The ductility of metallic materials is generally defined as the ability to deform plastically without fracture. It is usually expressed as a measure of the strain at fracture in a simple tension test¹. However, the percentage elongation in a tensile test is often dominated by the uniform elongation, which is dependent on the slope of the stress/strain curve. The end of uniform elongation coincides with the onset of plastic instability accompanied by voids nucleation, their growth and coalescence. It appears that the elongation value is too complex to be regarded as a fundamental property of a material and it seems reasonable to assume that any criterion of fracture will be based on some combination of stress and strain rather than on either of these quantities separately. Two grades of copper base alloys used for the production of commutators for electrical motors were tested in compressing and stretching. The bulk formability of these alloys were projected using the Cockcroft-Latham criterion^{2,3}, based on the tensile strain energy density at fracture. This criterion emphasizes the importance of tensile stresses in fracture and can be applied to a variety of cold working processes.

Key words: ductility, formability, fracture, Cockcroft-Latham fracture criterion, copper base alloys

Duktilnost kovinskih materialov je v splošnem definirana kot sposobnost, da se plastično deformirajo brez pojavljanja razpok. Običajno jo izrazimo z lomno deformacijo pri enostavnem nateznem preiskusu¹. V odstotkih izmerjen celokupni raztezek pri nateznem preiskusu je dokaj odvisen od enakomernega raztezka, to je od strmine krivulje napetost-deformacija. Konec enakomernega raztezanja sovпада s pojavljanjem plastične nestabilnosti, ki jo spremlja nastajanje por, njihova rast in združevanje. Zdi se, da je raztezek preveč kompleksen in ga ne moremo smatrati kot osnovno materialno lastnost. Zato je smiseln privzetek, po katerem bo moral lomni kriterij temeljiti prej na neki kombinaciji napetosti in deformacij, kot le na eni posamični količini. Za tlačno in natezno preiskovanje smo izbrali dve bakrovi zlitini za izdelavo kolektorjev pri elektromotorjih. Masivno preoblikovalnost teh zlitin smo opredelili s Cockcroft-Lathamovim kriterijem^{2,3}, ki temelji na gostoti natezne deformacijske energije. Ta kriterij poudarja pomen nateznih napetosti pri lomu in ga lahko uporabimo pri različnih procesih preoblikovanja v hladnem.

Ključne besede: duktilnost, preoblikovalnost, lom, Cockcroft-Lathamov kriterij loma, bakrove zlitine.

1. Introduction

The evolution of ductile damage within the deforming body is considerably influenced by the stress state in the material. It was suggested by Siebel⁴ that the cracking in metalworking is associated with induced tensile stresses, even in processes such as forging that are predominantly compressive. The importance of tensile stresses is indirectly confirmed by the large increase in ductility when the materials are deformed under hydrostatic pressure⁵. Pugh and Green⁶ demonstrated that superimposing a hydrostatic pressure in the extrusion process greatly enhanced

reductions could be achieved in ductile materials, and that even some brittle materials could be extruded without difficulty. In a tensile test of a cylindrical test specimen the stresses at the minimum section of the neck can be calculated in different ways^{5,7-11} and may be considered to be the sum of two parts. One part, the equivalent stress, is equal to the current yield stress and is constant across the cross-section. The other part, a hydrostatic tension, varies from zero at the periphery to a peak value at the centerline. As stated by Cockcroft and Latham³, that the use of the criterion based on total plastic work per unit volume at the fracture point, which would take into account only the equivalent stress i.e. the current yield stress, is not a proper solution.

* Dr. Boris ULE, dipl. inž.,
IMT Ljubljana, Lepi pot 11, 61000 Ljubljana

The current yield stress, unlike the peak stress, is not influenced by the shape of the necked region. Consequently, the neck shape should have no effect on the fracture strain, a conclusion which is contrary to experimental facts¹. Therefore Cockcroft² and Cockcroft and Latham¹ proposed a criterion based on the tensile strain energy density where the magnitude of the highest normal stress is taken into account. At tensile testing this would be the stress acting in the centerline where fracture is initiated.

As an outgrowth of experimental evidence of the influence of stress state on ductile fracture, several other criteria were also suggested for the prediction of fracture in complex stress states. A modification of the Cockcroft-Latham criterion which includes a hydrostatic-pressure term was suggested by Brozo et al.¹². Other criteria of importance were proposed by Oyane¹³, Cliff¹⁴, Hoffmann¹⁵ and Osakada¹⁶. Such criteria were successfully applied by a number of investigators to a variety of cold working operations¹⁷⁻²¹.

2. Fracture criterion

With the Cockcroft and Latham tensile ductility approach, the fracture is predicted when

$$\int_0^{\bar{\epsilon}_f} \bar{\sigma} (\sigma^* / \bar{\sigma}) d\bar{\epsilon} = C \tag{1}$$

where $\bar{\epsilon}$ is equivalent i.e. effective strain, $\bar{\epsilon}_f$ is equivalent strain at fracture, $\bar{\sigma}$ is equivalent i.e. effective stress, σ^* is the highest tensile stress, $(\sigma^*/\bar{\sigma})$ is a non-dimensional stress-concentration

factor representing the effect of the highest tensile stress, σ^* , and C is a material constant. If there is no tensile stress operating but only a compressive stress, $\sigma^* = 0$ and fracture does not occur¹.

The expression (1) has the dimensions of work per unit volume ($N/m^2 = Nm/m^3 = J/m^3$). The reduced form

$$\int_0^{\bar{\epsilon}_f} \sigma^* d\bar{\epsilon} = C \tag{2}$$

is used for calculation. The correction for necking and projections for σ^* could be obtained by different approaches^{5,7,11}. Wright and coworkers¹⁸, for instance, successfully used the equations of Davidenkov and Spiridonova⁷, whereas the equations of Bridgman⁵ were used in our experiments.

Fig. 1 illustrates the geometry at the necked region and the distribution of axial stress by this localized deformation. In accordance to Bridgman⁵, the variation of the stresses in a minimum section of a necked bar in tension is given as

$$\sigma_{av} = \bar{\sigma} (1 + 2\rho / R) \ln (1 + R / 2\rho) \tag{3a}$$

$$\sigma_{rr} = \sigma_{\theta\theta} = \bar{\sigma} \ln \frac{R^2 + 2R\rho - r^2}{2R\rho} \tag{3b}$$

$$\sigma_{zz} = \bar{\sigma} + \sigma_{rr} \tag{3c}$$

where σ_{av} is the average stress on the minimum section of the neck (load divided by minimum neck area), R is the radius of the minimum cross section at the neck, r' is the so called "strained length" ($r' \equiv r / R_0$), R_0 is the radius of initial cross section ($R_0 = 5$ mm) and ρ is the radius of curvature of the neck profile. In the centerline of the necked region, where $r = r' = 0$, $z = 0$ the stress component σ_{zz} reaches the highest value $\sigma_{zz,max} = \sigma^*$

$$\sigma^* = \bar{\sigma} + \bar{\sigma} \ln \frac{R + 2\rho}{2\rho} \tag{4}$$

Considering the strain hardening, the flow curve can be approximated by several constitutive equations. The most common are proposed by Hollomon²², Ludwik²³, Swift²⁴ and Voce²⁵. The most simple one is the Hollomon power law relation:

$$\bar{\sigma} = K \bar{\epsilon}^n \tag{5}$$

where n is the strain-hardening exponent and K is the strength coefficient of the material. Both constants could be determined simply by the values of 0.2% offset yield strength and fracture stress¹⁸ or by computer least-squares fits by plotting $\ln \bar{\sigma}$ against $\ln \bar{\epsilon}$, where n and K are the slope and intercept respectively. However, the strain-hardening exponent n , and the strength coefficient, K , could be also evaluated from the tensile test data by applying the criterion of instability at the onset of necking, $d\bar{\sigma}/d\bar{\epsilon} = \bar{\sigma}$. From this, it can be shown that at necking, where the ultimate tensile strength is measured, the strain-hardening exponent is given as

$$\bar{\epsilon}_n = n \tag{6}$$

Once the strain-hardening exponent is known, the strength coefficient K in the Eq. (5) can be easily determined by means of ultimate tensile strength σ_{ut} , as

$$K = \sigma_{ut} (2 \cdot 71828 / n)^n \tag{7}$$

From the results of Eq. (5), a relationship of σ^* to $\bar{\epsilon}$ can be determined by using Eqs. (3a) and (4) and assuming that the

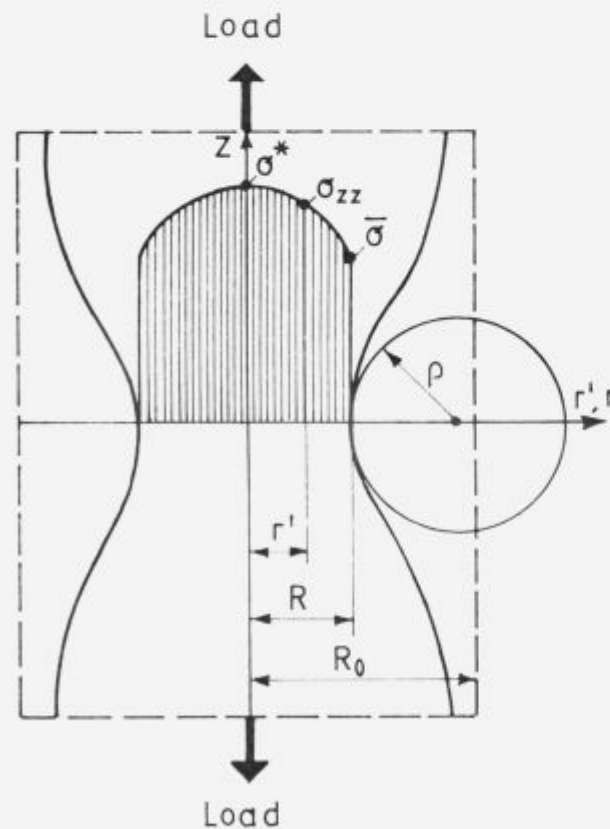


Figure 1: The geometry at the necked region and the distribution of axial stress σ_{zz} .

Slika 1: Geometrija vratu in porazdelitev aksialne napetosti σ_{zz} .

necking is initiated at the ultimate tensile strength σ_u , when $\sigma_u = \sigma_{n-1}$ and when $\bar{\epsilon}$ achieves n (Eq. 6), assuming also that σ^* increases linearly with equivalent strain (Fig. 2). Considering the hatched areas on Fig. 2, the integral (2) can be separated as follows

$$C = \int_0^{\bar{\epsilon}_0} \sigma^* d\bar{\epsilon} = \int_0^{\bar{\epsilon}_0} \bar{\sigma} d\bar{\epsilon} + \int_{\bar{\epsilon}_0}^{\bar{\epsilon}_f} \sigma^* d\bar{\epsilon} \quad (8)$$

By substituting the known function $\bar{\sigma}$ vs. $\bar{\epsilon}$ and using a trapezoidal formula for the second integral, we finally get

$$C = \frac{K}{n+1} \bar{\epsilon}_0^{n+1} + \frac{\sigma_{av,u} + \sigma_f}{2} (\bar{\epsilon}_f - \bar{\epsilon}_0) \quad (9)$$

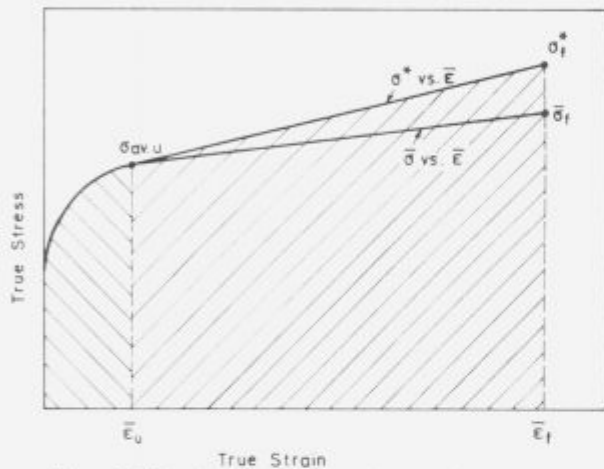


Figure 2: Effective stress, σ , and peak stress, σ^* , versus effective strain at tensile testing (schematically).

Slika 2: Ekvivalentna napetost σ in maksimalna napetost σ^* v odvisnosti od ekvivalentne deformacije pri natezanju (shematsko).

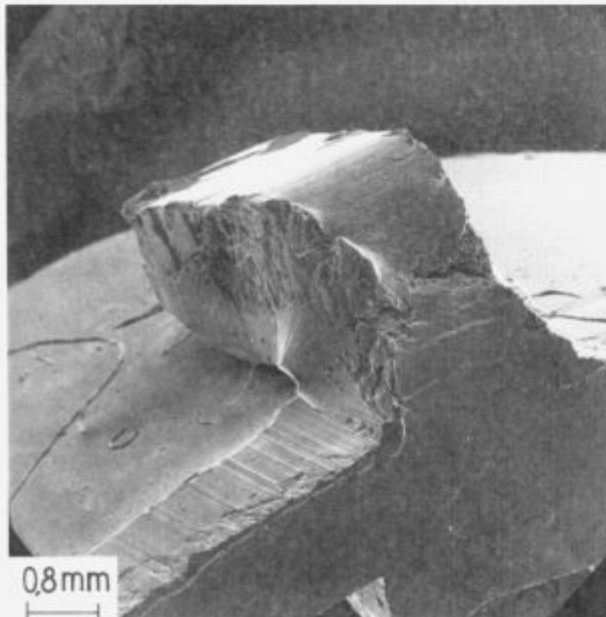


Figure 3: Cracks on commutator segments occurred at cold bending.

Slika 3: Razpoke, nastale na krakih kolektorja pri upogibanju v hladnem.

3. Experimental methods

Two copper base alloys declared as CuAg0.2 (OF) and CuAg0.2 respectively were selected for the present study. Both alloys, commercially available as one-half inch diameter wires, contain 0.2 wt. % Ag. This type of copper base alloys has good creep strength at elevated temperatures and high softening temperature and is used for instance for the production of commutators for electrical motors.

The experimental CuAg0.2 alloy contained 0.01 wt. % O and 0.005 wt. % P whereas the CuAg0.2 (OF) alloy i.e. oxygen free alloy contained < 0.005 wt. % O and 0.002 wt. % P. However, the bulk workability of CuAg0.2 alloy with higher oxygen content was essentially worse than that of oxygen free alloy. As shown on Fig. 3, a ductile damage occurred at cold bending of commutator segments from such oxygen containing CuAg0.2 alloy. On the contrary, the bulk formability of experimental oxygen free alloy was excellent as it didn't present any problems in metalworking processes.

The microstructure of both alloys is shown in Fig. 4 and 5. The microstructure of oxygen containing CuAg0.2 alloy (Fig. 4) consisted of relatively small grains with twinned areas, whereas the microstructure of oxygen free CuAg0.2 alloy (<0.005 % O) (Fig. 5) is characterized by somewhat larger, equiaxed grains

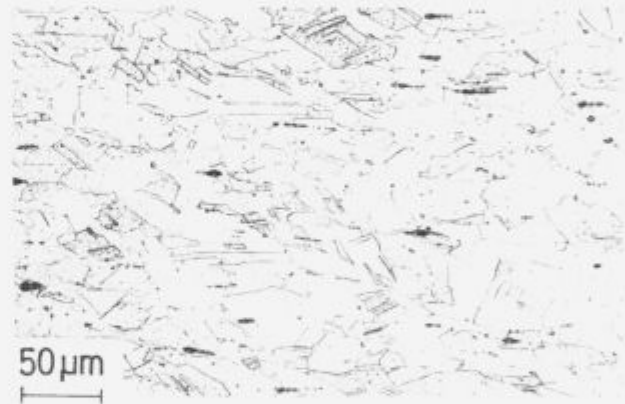


Figure 4: Microstructure of oxygen containing CuAg0.2 alloy, showing relatively small grains with some twinned areas.

Slika 4: Mikrostruktura kisik vsebujoče zlitine CuAg0.2. Razmeroma drobna kristalna zrna s posameznimi področji dvojčenja.

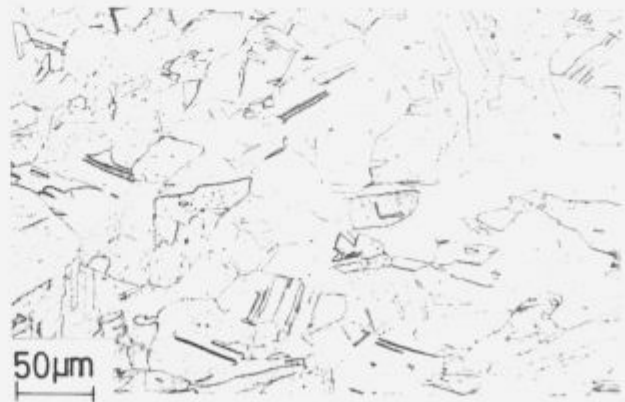


Figure 5: Microstructure of oxygen free CuAg0.2 alloy, showing equiaxed grains with irregular boundaries. Some grains contain twinned areas.

Slika 5: Mikrostruktura kisika proste zlitine CuAg0.2. Enakoosna kristalna zrna z iregularnimi mejami in dvojčki v posameznih zrnih.

with irregular boundaries and twinned areas. The microstructure of both alloys is typical for the as annealed state where only a slight cold reduction was applied at the calibration drawing.

Tensile flow curves were obtained using an Instron machine by pulling standard tensile specimens with gauge sections of 10 mm diameter and 100 mm length at a cross-head speed of 1 mm/min. The neck profile radius was established from the photographs of the necked region using an appropriate geometrical approximation. A discontinuous compression testing was carried out on a instrumented hydraulic press on specimens with 10 mm in diameter and initial height of 12 mm. In order to minimize the frictional constraints, teflon was used on contact surfaces and constant friction coefficient of 0.024 was achieved. Cumulative height reductions reached 86 %. The strain rate at compression testing was comparable with that at the uniform tension and remained nearly constant over most of the strain range. Load-displacement data obtained were fed into a computer by points for stress-strain analysis. A correction factor for the adequate compensation of friction was also incorporated into the computer program.

4. Results

Fig. 6 are the plots of load vs. elongation at tensile test of both experimental alloys. The values obtained at testing are listed in **Table I**. The yield stress at tensile testing was determined as 0.2 % Offset Yield Stress. The yield stress measured at compression testing is also included in the table (values in parenthesis). As already mentioned, the radius of the minimum cross section of the neck *R*, and the radius of curvature of the neck profile *r*, of the tensile specimens were measured too. By the CuAg0.2 alloy (0.01 % O) the neck profile radius was 2.20 mm, the minimum cross section radius was 2.85 mm, whereas at oxygen free CuAg0.2 alloy (<0.005 % O), where more a rupture than a fracture was observed, the neck profile radius was only 0.15 mm and the minimum cross section radius was 1.80 mm.

In **Table II** the values of Hollomon constants calculated from the compression- and tensile tests data are listed. The constants, obtained from tensile test data were determined by various methods of analysis, because the high percent error in $\bar{\epsilon}_u$ makes sometimes the Eq. (6) unacceptable. However, *n* is the exponent of an empirical equation (5) and it is not surprising that this equation cannot accurately describe the stress-strain curves in the whole strain range. Man et al.²⁶ described the tensile curves

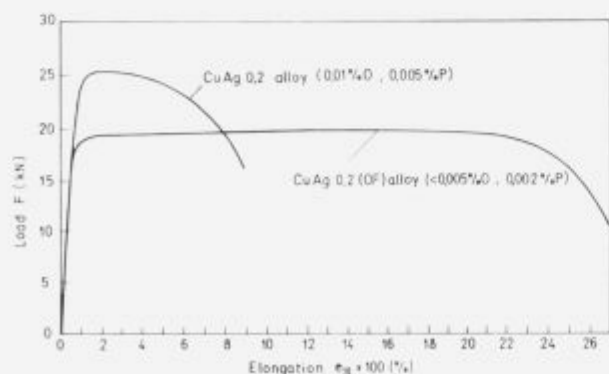


Figure 6: Load vs. elongation at tensile test of both experimental alloys.

Slika 6: Odvisnost med obremenitvijo in raztezkom pri nateznem preizkušanju obeh eksperimentalnih zlitin.

Table I: Tensile test results

Tabela I: Rezultati nateznega preizkušanja

	Yield stress* σ_{ys} (MPa)	Tensile strength σ_{ts} (MPa)	Uniform elongation $\epsilon_u \times 100$ (%)	Total elongation $\epsilon_{10} \times 100$ (%)	Reduction in area $Z \times 100$ (%)
CuAg0.2 alloy (0.01 % O)	306 (321)	323	2	9	68
CuAg0.2 (OF) alloy (<0.005%O)	232 (248)	258	14.2	27	87

*The values in parenthesis were obtained by compression testing

Table II: Comparison of Hollomon constants by various test methods

Tabela II: Primerjava Hollomonovih konstant dobljenih pri različnih metodah preizkušanja

	Strength coefficient <i>K</i> (MPa)	Strain-hardening exponent <i>n</i>	Correlation coefficient <i>r</i>
Compression Test			
CuAg0.2 alloy (0.01 % O)	397	0.090	0.977
CuAg0.2 (OF) alloy (<0.005 % O)	379	0.139	0.993
Tension test			
CuAg0.2 alloy (0.01 % O)	431	0.087*	
CuAg0.2 (OF) alloy (<0.005 % O)	385	0.133**	

*Calculated from the true stress-true strain tensile test data

**Calculated from the uniform elongation /Eq. (6)/

Table III: Values of the material constants

Tabela III: Vrednosti materialnih konstant

	σ_{ys} (MPa)	σ_{ts} (MPa)	$\bar{\epsilon}_u$	$\bar{\sigma}_f$ (MPa)	$\bar{\epsilon}_f$	σ'_f (MPa)	C/Eq(9) (MJ/m ³)
CuAg0.2 alloy (0.01 % O)	306	330	0.019	435	1.124	652	548
CuAg0.2(OF) alloy (<0.005 % O)	232	288	0.129	423	2.040	1246	1499

of copper using two equations of Hollomon type²⁷. This kind of analysis is based on the assumption that a change in deformation mechanism occurs during the deformation.

The collection of final results is given in **Table III** where 0.2 % offset yield stress, σ_{ys} , average ultimate stress, σ_{ts} , and fracture stress, σ_f , with corresponding strains, $\bar{\epsilon}_u$ and $\bar{\epsilon}_f$ respectively, the highest tensile stress σ'_f as well as the material constant C are shown. The value of C, i.e. the value of tensile strain energy density of oxygen free CuAg0.2 alloy (<0.005 % O) is extremely large. This alloy with low oxygen content exhibited

more a rupture than a fracture at tensile testing resulting in adequate small radius of curvature of the neck profile while the tensile stress in necked region strongly increased. In spite of the fact that the original Bridgman⁵ analysis and the similar analysis of Davidenkov and Spiridonova⁷ give the best approximate procedure for the calculation of stress distribution in the necked region, nowadays, more accurate numerical solutions can be obtained with FEM.

5. Discussion

Using the fracture criterion based on the model of Cockcroft and Latham^{2,3}, the tensile strain energy density at fracture for two copper base alloys was calculated. The calculation utilized the results of tensile and compression tests. When the constant cross-head-speed is used at tensile test, the strain rate decreases slightly during the homogenous deformation and then rises rapidly as necking occurs. The rise in strain rate during the necking results in an anomalous rise in flow stress and restricts the usefulness of the data obtained by strains smaller than those prevailing during the onset of the necking²⁷. Probably some discrepancies between the tensile and the compression test results (see **Table II**) could be explained also with Bauschinger effect and with the assumption that a change in deformation mechanism occurs during tensile deformation. Zankl²⁸ and Schwink and Vorbrugg²⁹ found these kind of stages also in the tensile curves of annealed nickel and copper at low strains. Furthermore, Mishra et al.³⁰ proposed that in the range of uniform strain the Hollomon law overestimates the flow stress in the initial stages and underestimates it in the final stages. It seems therefore, that the tensile test data of experimental copper base alloys should fit better with double-n method which uses the two Hollomon equations. Kleemola and Nieminen³¹ found out that the use of the Hollomon equation for pure copper in an annealed state and after 40 pct deformation gives a misleading picture of the strain-hardening properties of the material because the strain-hardening exponent n is not equal to the correct $\bar{\epsilon}_c$ value. The same was also observed in our CuAg0.2 experimental alloy with 0.01 % oxygen where computer least-squares fits by plotting tensile test data had to be used instead of Eq. (6). In opposition to tensile test data, the compression test data are obtained from a much larger strain range and it is therefore assumed that the use of the simple Hollomon power law relation is justified. The regression analysis of compression test data also gives satisfactory high linear correlation coefficients (0.98 and 0.99 respectively).

The data presented in **Table III** (C-values) shows that at oxygen free CuAg0.2 alloy the integral of the maximal tensile stress over the plastic strain path /Eq. (9)/ reaches a value of approx. 1500 MJ/m³, which is nearly three times larger than that of CuAg0.2 alloy with 0.01 % oxygen (C approx. 550 MJ/m³). However, the reduction in area at tensile test of oxygen free CuAg0.2 alloy is only for one quarter larger than that of CuAg0.2 alloy with 0.01 % oxygen. It seems that a considerable increase in ductility may result by an only relatively low improvement in the reduction-in-area value, so that such way of expressing the ductility shows little discrimination in very ductile metals. Namely, once the necking develops, a "negative feedback" effect occurs, which tends to prevent the exhibition of really large ductility values¹. At the onset of necking, the stress system changes and a component of hydrostatic tensile stress is generated which is superimposed on the axial stress. The hydrostatic tensile stress increases as the neck becomes deeper, with the result that the fracture is more likely to occur. This situation leads

to a stabilizing effect and an increase in ductility causes a deeper neck to be formed, hence higher local stresses are developed and a greater possibility of fracture occurs. The Cockcroft-Latham criterion of ductile fracture is therefore a much more reasonable criterion than the criterion based simply on reduction-in-area value at tensile test. However, it should be noticed that at the neck profile which is characteristic for rupture instead of fracture, the extremely high value of tensile stress σ^* , and high tensile strain energy density C , are somewhat doubtful. The equations of Bridgman⁵ / (3a,b and c) and (4)/ and equations of Davidenkov and Spiridonova⁷ becomes questionable at very low radius of curvature of the neck profile typical for the rupture and when asymptotic continuum mechanics analyses could not be applied for the description of stress state due to local singularity.

The excellent bulk formability of the experimental CuAg0.2 oxygen free alloy with regard to the verification based on the Cockcroft-Latham criterion is not surprising. This criterion has the desirable feature for homogenous compression, in which case the tensile stress σ^* is zero and no fracture limit is predicted. This coincides well with the experimental results at homogeneous (frictionless) compression. However, following the theoretical analysis of Kuhn et al.¹, it is possible to relate the C-value calculated from tensile test data /Eq. (9)/ and the principal tensile and compressive surface strains, i.e. the circumferential and axial strains measured on the barreled equatorial free surface at fracture in upset test. It was also experimentally confirmed that there is a linear relationship between the tensile and compressive surface strains at fracture by upsetting by rolling and by bending. Consequently, the representation of fracture data as a plot of tensile versus compressive strains at fracture became a useful form for the analysis of the fracture in cold forming processes resulting in a "forming limit diagram concept". The Cockcroft-Latham tensile strain energy fracture criterion is consistent with this concept¹.

6. Conclusions

The Cockcroft-Latham tensile strain energy density criterion was used for a reliable evaluation of the ability of two copper alloys to metalworking operations. This criterion implies that the fracture depends both on the stresses imposed and on the strains developed and it could be described as "fracture will occur when the plastic work of the largest tensile stress, per unit volume, reaches a characteristic critical value".

It was demonstrated that there is a good qualitative agreement between the prediction of formability under bulk metalworking conditions based on this criterion and the observed behaviour in the production of commutators for electrical motors. The plastic work done per unit volume by oxygen free CuAg0.2 alloy with excellent bulk formability is nearly three times larger than that done by the oxygen containing CuAg0.2 alloy (0.01 % O), while the difference in the tensile reduction of area of both alloys was much smaller. Consequently, the reduction-in-area value at tensile test cannot be appreciated in general.

References:

- 1 Kuhn, H. A., Lee, P. W., Erturk, T.: *Trans. ASME*, 1973, 213-218.
- 2 Cockcroft, M. G.: *Ductility*, American Society for Metals, Metals Park, Ohio, 1968, 199-226.
- 3 Cockcroft, M. G., Latham, D. J.: *Journal of the Institute of Metals*, 96, 1968, pp. 33-39. ⁴ Siebel, E.: *Steel*, 93, 1933, 17, 37.

- ⁵ Bridgman, P. W.: *Studies in Large Plastic Flow and Fracture*, McGraw-Hill, New York, 1952.
- ⁶ Pugh, H. L. D., Green, D.: The Effect of Hydrostatic Pressure on the Plastic Flow and Fracture of Metals, *Proc. Inst. Mech. Eng.*, 179, 1964, No. 1.
- ⁷ Davidenkov, N. N., Spiridonova, N. I.: *Proc. Amer. Soc. Test. Mat.*, 46, 1946, 1147.
- ⁸ Chen, W. H.: *International Journal for Solids and Structures*, 7, 1971, 685-717.
- ⁹ Needleman, A.: *Journal for Mechanics and Physics of Solids*, 20, 1972, 111-127.
- ¹⁰ Norris, D. M. jr., Moran, B., Schudder, J. K., Quinones, D. F.: *Journal for Mechanics and Physics of Solids*, 26, 1978, 1-17.
- ¹¹ Saje, M.: *Int. J. Solids Structures*, 15, 1979, 731-742.
- ¹² Brozzo, P., Deluca, B., Rendina, R.: A new method for the prediction of the formability limits of metal sheets, *Proceedings of 7th Biennial Congr. of Int. Deep Drawing Research Group*, 1972 (from Dood, B. and Bai, Y.: *Ductile Fracture and Ductility*, Academic Press inc., London, 1987, 205.)
- ¹³ Oyane, M.: *Bull. JSME*, 15, 1972, 1507-1513.
- ¹⁴ Clift, S. E.: Identification of defect locations in forged products using the finite element method, *Ph.D.-Thesis*, Univ. of Birmingham, U.K., 1986.
- ¹⁵ Hoffmanner, A. L.: *Metal Forming - Interrelationship Between Theory and Practice*, A. L. Hoffmanner, ed., Plenum Press, New York, 1971, 349-391.
- ¹⁶ Osakada, K., Koshijima, J., Sekiguchi, H.: *Bull. JSME*, 24, 1981, 534-539.
- ¹⁷ Bolt, P. J., Kals, J. A. G., Dautzenberg, J. H.: Prediction of ductile failure in forming, *Proceedings of the Second International Conference on Technology of Plasticity*, Vol. I, Stuttgart, August 1987, 385-391.
- ¹⁸ Wright, R. N., Kircher, T. A., Vervlied, J. R.: *Journal of Metals*, October 1987, 26-29.
- ¹⁹ Dung, N. L., Mahrenholtz, O.: A Criterion for the Ductile Fracture in Cold Forging, *Proceedings of the Second International Conference on Technology of Plasticity*, Vol. II, Stuttgart, August 1987, 1013-1020.
- ²⁰ Vujović, V., Vilotić, D., Plančak, M., Trbojević, I., Francuski, P.: Strain history influence on the material formability, *Proceedings of the Fourth International Conference on Technology of Plasticity*, Vol. I, Beijing, China, September 1993, 275-280.
- ²¹ Luo, Z. J., Ji, W. H., Guo, N. C., Xu, X. Y., Xu, Q. S., Zhang, Y. Y.: A ductile-damage model and its application to metal-forming processes, *Journal of Materials Processing Technology*, Vol. 30, 1992, 31-43.
- ²² Hollomon, J. H.: *Trans. AIME*, 162, 1945, 268-290.
- ²³ Ludwik, P.: *Elemente der Technologischen Mechanik*, Verlag Von Julius Springer, Leiptzig, 1909, 32.
- ²⁴ Swift, H. W.: *Journal Mech. Phys. Solids*, Vol. I, 1952, 1-18.
- ²⁵ Voce, E.: *Journal Inst. Met.*, 74, 1948, 537-562.
- ²⁶ Man, J., Holzmann, M., Vlach, B.: *Phys. Status Solidi*, 19, 1967, 543-553.
- ²⁷ Rao, K. P., Doraivelu, S. M., Gopinathan, V.: *Journal of Mechanical Working Technolgy*, No. 6, 1982, 63-88.
- ²⁸ Zankl, G.: *Z. Naturforsch.*, 18a, 1963, 795-809.
- ²⁹ Schwink, Ch., Vorbrugg, W.: *Z. Naturforsch.*, 22a, 1967, 624-642.
- ³⁰ Mishra, N. S., Mishra, S., Ramaswamy, V.: *Metallurgical Transactions A*, 20A, 1989, 2819-2829.
- ³¹ Kleemola, H. J., Nieminen, M. A.: *Metallurgical Transactions A*, 5, 1974, 1863-1866.